Muscle-specific RING finger-2 (MURF-2) is important for microtubule, intermediate filament and sarcomeric M-line maintenance in striated muscle development

Abigail S. McElhinny[1,*], Cynthia N. Perry[1], Christian C. Witt[3], Siegfried Labeit[3] and Carol C. Gregorio[1,2]

[1]Department of Cell Biology and Anatomy and [2]Department of Molecular and Cellular Biology, University of Arizona, Tucson, AZ 85724, USA
[3]Institut für Anästhesiologie und Operative Intensivmedizin, Universitätsklinikum 68135 Mannheim, Germany
*Author for correspondence (e-mail: abigailm@email.arizona.edu)

Accepted 13 February 2004
Journal of Cell Science 117, 3175-3188 Published by The Company of Biologists 2004
doi:10.1242/jcs.01158

Summary

The efficient functioning of striated muscle is dependent upon the structure of several cytoskeletal networks including myofibrils, microtubules, and intermediate filaments. However, little is known about how these networks function together during muscle differentiation and maintenance. In vitro studies suggest that members of the muscle-specific RING finger protein family (MURF-1, 2, and 3) act as cytoskeletal adaptors and signaling molecules by associating with myofibril components (including the giant protein, titin), microtubules and/or nuclear factors. We investigated the role of MURF-2, the least-characterized family member, in primary cultures of embryonic chick skeletal and cardiac myocytes. MURF-2 is detected as two species (~55 kDa and ~60 kDa) in embryonic muscle, which are down-regulated in adult muscle. Although predominantly located diffusely in the cytoplasm, MURF-2 also colocalizes with a sub-group of microtubules and the M-line region of titin. Reducing MURF-2 levels in cardiac myocytes using antisense oligonucleotides perturbed the structure of stable microtubule populations, the intermediate filament proteins desmin and vimentin, and the sarcomeric M-line region. In contrast, other sarcomeric regions and dynamic microtubules remained unaffected. MURF-2 knock-down studies in skeletal myoblasts also delayed myoblast fusion and myofibrillogenesis. Furthermore, contractile activity was also affected. We speculate that some of the roles of MURF-2 are modulated via titin-based mechanisms.

Key words: MURF, Titin, Microtubules, Myofibrils, M-line, Myofibrillogenesis

Introduction

The efficient functioning of striated muscle is dependent upon the precise interactions and alignment of complex cytoskeletal networks. For example, sarcomeres, the basic contractile units of myofibrils, are comprised of uniformly arranged filament systems and regulatory proteins. The actin-containing thin filaments are anchored in the Z-lines and extend toward the middle of the sarcomere, the M-line, where they interact with the myosin-containing thick filaments to drive contraction. A third filament system is composed of single molecules of titin, the largest known vertebrate protein (~3.7 MDa). Titin filaments span half sarcomeres, with their N-termini overlapping in the Z-lines and their C-termini overlapping in the M-lines, thus forming a continuous filament system among adjacent myofibrils (Obermann et al., 1996; Gregorio et al., 1998; Mues et al., 1998). Based on the assembly properties, molecular layout and modular structure of titin, it is proposed to act as a template for myofibrillogenesis. Additionally, the I-band region contains elastic elements that contribute to muscle stiffness (Linke and Granzier, 1998; Granzier and Labeit, 2002 and references therein). Intriguingly, the C-terminal region contains a unique Ser/Thr kinase domain of unknown function, and recent studies have identified various signaling molecules associated with the giant molecule (Labeit and Kolmerer, 1995; Sorimachi et al., 1995; Young et al., 2001; Bang et al., 2001; Centner et al., 2001; Miller et al., 2003). Thus, titin has multiple roles in muscle, potentially including signaling pathways involved in myofibril assembly.

Although much has been discovered recently concerning sarcomeric protein interactions and functions, relatively little is known about how myofibrils are connected to other cytoskeletal arrays (including microtubules, intermediate filaments, and costameres), organelles, and neighboring myocytes (reviewed in Clark et al., 2002). Furthermore, the function of the non-contractile cytoskeletal arrays in muscle development and maintenance remains unclear, although mounting evidence suggests a role in muscle differentiation and function. For example, perturbation of microtubule dynamics with depolymerizing or stabilizing agents inhibits skeletal myoblast fusion, differentiation, and normal myofibrillogenesis (Antin et al., 1981; Toyama et al., 1982; Saitoh et al., 1988). In the heart, disruption of microtubules alters cytoplasmic viscosity, myosin mRNA transport, Ca^{2+} signaling, and gene expression (Perhonen et al., 1998; Takahashi et al., 1998; Gomez et al., 2000; Calaghan et al., 2001; Kerfant et al., 2001). Furthermore, microtubules are required for proper contractile function and their levels increase in animal models of pressure-overload cardiac hypertrophy (Klein, 1983; Tsutsui et al., 1993). Investigations into the mechanisms by which microtubules function in muscle

are challenging as their distinct arrays and orientations vary among muscle types, during development, and with disease (Saitoh et al., 1988; Gundersen et al., 1989; Kano et al., 1991; Boudriau et al., 1993; Webster, 1997; Belmadani et al., 2002).

In striated muscle, intermediate filament proteins (including desmin, vimentin, nestin, paranemin, synemin and cytokeratins) have various subcellular localizations, including at the Z-line region, costameres, intercalated discs and myotendinous junctions. Therefore, they may link myofibrils to the sarcolemma, organelles and neighboring myocytes (Granger and Lazarides, 1979; Holtzer et al., 1985; Milner et al., 2000; O'Neill et al., 2002) (see Clark et al., 2002 for review). In particular, intermediate filaments are thought to be involved in maintaining muscle stability as desmin-null mice exhibit a reduction of myofibril alignment, significant muscle degeneration and necrosis, and impaired force transmission (Milner et al., 1996; Li et al., 1997; Milner et al., 1999; Balogh et al., 2002). Exactly how the intermediate filaments assemble during development is not understood, although some require a specific subpopulation of microtubules – detyrosinated microtubules (Glu-MTs) – for their localization and integrity in some cell types (Gurland and Gundersen, 1995; Kreitzer et al., 1999).

Recently, a novel family of muscle RING finger (MURF) proteins was identified whose members associate with myofibrils and/or microtubules. Structurally, the three known MURFs (MURF-1, -2, and -3; also known as RNF 28, 29, and 30) are members of the RING finger-B box-coiled-coiled (RBCC) family, a group of proteins implicated in ubiquitination and signal transduction (Spencer et al., 2000; Centner et al., 2001). All MURF members homo- and hetero-oligomerize, apparently via their coiled coil domains, although the functional implications of this are not known (Centner et al., 2001). MURF-1 is a titin-binding protein, specifically interacting with the C-terminal immunoglobulin (Ig) domains, A168-A170, adjacent to the titin kinase domain (Centner et al., 2001). MURF-1 also binds small ubiquitin-related modifier-3 (SUMO-3/SMT3b) and the transcription factor, glucocorticoid modulatory element binding protein-1 (GMEB-1) (Dai and Liew, 2001; McElhinny et al., 2002). MURF-1 is important for maintaining the integrity of the M-line region in titin and thick filaments in cardiac myocytes (McElhinny et al., 2002). Furthermore, conditional expression of truncated titin missing the kinase domain and the MURF-1-binding region results in sarcomeric disassembly and muscle weakness in mice (Gotthardt et al., 2003), and the skeletal muscles of MURF-1 null mice are more resistant to atrophy (Bodine et al., 2001). Taken together, these data suggest that MURF-1 participates in the regulation of myofibril maintenance and turnover; exactly how the binding partners of MURF-1 and their emerging potential pathways (i.e. ubiquitination, sumoylation, steroid-regulation) are involved in these processes remains unknown.

MURF-3 is developmentally up-regulated and its ectopic expression in COS cells stabilizes microtubules. Ablation of its expression in C2C12 skeletal muscle cells inhibits the accumulation of detyrosinated microtubules and blocks myogenic events (Spencer et al., 2000). MURF-3 therefore may play a role in establishing or maintaining the stable microtubule array known to be required for muscle differentiation (Gundersen et al., 1989; Chang et al., 2002). Finally, MURF-2 mRNA transcripts are down-regulated during development, and based on its in vitro hetero-oligomerization with MURF-1 (Centner et al., 2001) and its transient localization patterns in skeletal myogenic cell lines (Pizon et al., 2002), it is proposed to act as an adaptor between microtubules, myosin, and titin during myofibrillogenesis. However, studies examining the function of MURF-2 in striated muscle are lacking.

Here, we aimed to investigate the functional properties of MURF-2 using two complementary model systems. First, primary cultures of embryonic chick cardiac myocytes have proven to be a powerful tool for investigating the functional properties and interactions of many cytoskeletal proteins in the context of living cells. However, as the cells are harvested from embryonic hearts that are already beating, this system is not ideal for deciphering specific events involved in muscle differentiation. Hence, we also investigated the localization and functional roles of MURF-2 in primary cultures of embryonic chick skeletal myocytes, where presumptive myoblasts withdraw from the cell cycle, fuse, undergo de novo myofibrillogenesis, and differentiate into mature myotubes (see Gregorio and Antin, 2000). We found that knock-down of MURF-2 mRNA and protein levels in cardiac myocytes specifically disrupted the integrity of the stable microtubule populations (Glu-MTs and Ac-MTs), the intermediate filament proteins desmin and vimentin, and the M-line region of the sarcomere (including myomesin and the C-terminal region of titin). Knock-down of MURF-2 levels in chick embryonic skeletal myoblasts also delayed fusion events and myofibrillogenesis. The observed perturbations were rescued upon co-transfection with human MURF-2-GFP constructs in both cell types. Our data indicate that MURF-2 has many subcellular localizations and has multiple roles in cardiac and skeletal myocytes; its proper expression is important for dynamic intermediate filament, microtubule and M-line based protein assembly.

Materials and Methods

Anti-MURF-2 antibodies and western blots

To investigate MURF-2 protein expression, affinity-purified rabbit polyclonal antibodies were generated against the KHL-coupled synthetic peptide derived from the extreme 17 C-terminal amino acid residues of mouse MURF-2 (NH_2-CPARHVFSFSWLNSLNE-COOH) and also against a recombinant fragment encompassing an internal, 83-residue fragment of mouse MURF-2 (Biogenes, Berlin). For details on expression methods in *E. coli*, see www.titin.org.

Western blots of striated muscle lysates were probed with the anti-MURF-2 antibodies essentially as described (Bang et al., 2001). For antibody characterization, rat heart lysate (snap-frozen tissue from fetal or adult hearts) was ground into a fine powder in liquid nitrogen using a mortar and pestle, and solubilized with 2× SDS sample buffer. Chick skeletal and cardiac myocyte cultures and skeletal myoblasts were directly solubilized in 2× SDS sample buffer. The lysates were fractionated by either 8% or 10% SDS-PAGE and transferred to nitrocellulose membranes. Nitrocellulose strips were stained with Ponceau S and strips containing equal amounts of actin were compared by western blotting. For detection of MURF-2 in antisense-treated cells, cardiac myocytes were solubilized 48 hours after antisense treatment with 9.2 M urea, and protein assays were performed to ensure equal loading (BCA Protein Assay kit, Pierce). The lysates were mixed with 2× SDS sample buffer for SDS-PAGE, transferred to nitrocellulose, and probed with the anti-

MURF-2 antibodies. Additionally, separate experiments were performed using 2× SDS sample buffer for solubilization of the cell culture lysates, as described above, and identical results were obtained. Notably, although a significant decrease in MURF-2 levels was consistently detected using NIH image, no significant change was observed for α-actinin (data not shown). Around 1 μg/ml of the anti-MURF-2 antibodies were used to probe the membranes for one hour at 4°C, followed by HRP-conjugated goat anti-rabbit IgG, for 1 hour at 4°C (1:25,000: Jackson ImmunoResearch Laboratories). The membranes were then incubated in SuperSignal chemiluminescent substrate (Pierce Chemical Co.) according to manufacturer's instructions and exposed to Biomax MR film (Eastman Kodak Co.).

Cell culture, transfection, and antisense oligonucleotide treatment

Cardiac myocytes were isolated from fetal rat and day-6 embryonic chick hearts and maintained as described (Gustafson et al., 1987; Gregorio and Fowler, 1995). Isolated cells were plated in 35-mm tissue culture dishes for RT-PCR analysis, or in dishes containing 12-mm diameter coverslips for immunofluorescence staining (~10^6 cells/dish). 15-20% of the cells in our primary cultures were fibroblasts. For MURF-2 antisense oligonucleotide treatment, the cardiac myocytes were not treated until day 3 to decrease toxicity. 10 μg of control or antisense oligonucleotide were added to 7 μl of Cytofectene (Biorad) and the DNA-lipid complex was incubated in 200 μl OptiMEM for 15 minutes at 37°C. Our transfection efficiency was >80% and over 20 cultures were analyzed. For cultures of chick cardiac myocytes, four 16-mer antisense oligonucleotides were designed using MURF-2 EST sequences from the BBSRC ChickEST Database (Boardman et al., 2002), three of which significantly knocked down MURF-2 levels: 5′-GCATAACCTGTGCAGG-3′ (B), 5′-GCAGACGACAGAAGGA-3′ (C), and 5′-GGTGCCACAAAA-GACT-3′ (D). For control oligonucleotides, reverse (but not complementary) sequences to the antisense oligonucleotides were used. We also designed four antisense oligonucleotides to the human MURF-2 cDNA sequence for use in rat myocytes, which yielded identical results as in chick myocytes (data not shown): 5′-GCACAACCTGTGTAGG-3′ (B), 5′-GCTACTTCTCAGATTG-3′ (C), 5′-CTCGCCATATCTTCTC-3′ (D). For expression of human GFP-MURF-2 fusion proteins in rescue experiments, full-length p60 MURF-2 cDNA was amplified by PCR with an 180S/1520R primer pair (see www.titin.org). The 1.6-kb inserts were cloned into pEGFP-C1, and 4 μg were co-transformed into myocytes with the chick MURF-2 antisense oligonucleotides.

For skeletal myotube cultures, myoblasts were isolated from day-11 chick embryo pectoralis muscle with modifications to previously described protocols (Almenar-Queralt et al., 1999; Ojima et al., 1999). In brief, muscle was dissected from 3-4 embryos and minced in ice-cold PBS. The minced tissue was suspended in 10 ml trypsin/EDTA (Life Technologies) and incubated for 10-15 minutes at 37°C, with intermittent pipetting to create a cell suspension. After centrifugation, the pellets were resuspended in growth medium: MEM with 15% chick embryo extract, 10% horse serum, 3 mM L-glutamine, and penicillin/streptomycin and filtered through cell strainers. The cells were incubated at 37°C for 1 hour on 100-mm tissue culture dishes to enrich for myoblasts. The collected cells were plated in growth medium at 4×10^5 cells/35-mm culture dish, containing 12-mm diameter coverslips coated with rat tail collagen (Sigma). Cells were transfected with antisense or control oligonucleotides during the pre-plating stage, using the conditions described above. By day 3 in culture, the cells were treated with 1-[beta-D-arabinofuranosyl]-cytosine (ara-C) (1 μg/ml) in differentiation medium: MEM containing 2.5% chick embryo extract, 10% horse serum, 3 mM L-glutamine and penicillin/streptomycin. Cells were fed every other day for a total culture period of 5-6 days. Myotubes were fixed in methanol at –20°C for 10 minutes.

RT-PCR analysis of MURF-2 mRNA transcripts

For amplification of MURF-2 mRNA transcripts, cultures were harvested for total RNA immediately after treatment with oligonucleotides, using a RNeasy Mini kit (Qiagen). cDNA was prepared from 20 μl of total RNA using the Super ScriptII Reverse Transcriptase (Invitrogen), and the cDNA concentration was determined using an Eppendorf Biophotometer. 100 ng of template were used per PCR reaction. Chick MURF-2 and MURF-3 primers were used for amplification in 25 μl reactions using Qiagen PCR kits: S: 5′-GGCTACAAGTCCTTCTCCAAAGAGC-3′ and R: 5′-CGTTTGTGAGAGGAGCAACCTGAC-3′ for MURF-2 (475-bp product); and S: 5′-CCAACCCGCTGTGGCAGTCGCG-3′ and R: 5′-CGCTCTTTTGGCGCTGGTACACGG-3′ for MURF-3 (348-bp product). Chicken glyceraldehyde-3-phosphate dehydrogenase (GAPDH) also was amplified as a loading control: S: 5′-GGCACTGTCAAGGCTGAAAACG-3′ and R: 5′-GGAGATGA-GATGATACCACGCTTAG-3′ (202-bp product). All PCR products were sequenced for verification.

Indirect immunofluorescence microscopy

Cells were stained essentially as described previously (Gregorio et al., 1998). Myocytes were fixed in methanol at –20°C for 10 minutes, washed in PBS, and incubated in 2% BSA, 1% normal donkey serum/PBS for 30-45 minutes to minimize nonspecific binding of antibodies. Cells were incubated with affinity-purified anti-MURF-2 antibodies (~10 μg/ml), followed by Texas Red-conjugated goat anti-rabbit IgG (1:600). Anti-tubulin antibodies included: anti-α-tubulin clone DM1A (at 1:500), anti-Tyr tubulin clone TUB-1A2 (at 1:1000), and anti-acetylated-tubulin clone 6-11B-1 (at 1:2000) antibodies (Sigma-Aldrich). Anti-Glu-tubulin polyclonal antibodies (SG) were a generous gift of J. Chlöe Bulinski (Columbia University, New York). For intermediate filament proteins, monoclonal anti-desmin clone D3 (1:2 of culture supernatant) (Developmental Studies Hybridoma Bank, University of Iowa), monoclonal anti-desmin clone DE-U-10 (1:200; Sigma-Aldrich), pre-diluted polyclonal anti-desmin (Biomeda), anti-vimentin clone VIM-13.2 (at 1:200) (Sigma-Aldrich), and anti-vimentin clone V9 (1:1000; Sigma-Aldrich) antibodies were used. Well characterized antibodies to sarcomeric components included: anti-myosin F59 (1:20 of culture supernatant) (generously provided by F. Stockdale, Stanford University, Stanford, CA), rabbit anti-titin A168-170 (at 1:200) (Centner et al., 2001), titin AB5 (1:3 of culture supernatant) (generously provided by J. Trinick, University of Leeds, U.K.), and monoclonal anti-myomesin B4 antibodies (1:50 of culture supernatant) (generously provided by J.-C. Perriard and E. Ehler, Swiss Federal Institute of Technology, Zurich, Switzerland) (Grove et al., 1984). For secondary antibodies, goat anti-mouse 488 (1:1000), goat anti-mouse Texas Red (1:600) or donkey anti-rabbit Texas Red (1:600) antibodies were used. All secondary antibodies were purchased from Jackson ImmunoResearch Laboratories and Molecular Probes. Phalloidin-350 (Molecular Probes) was used in triple-staining experiments in cardiac myocytes fixed in 2% paraformaldehyde/PBS for 15 minutes at room temperature. To label nuclei, cells were incubated in a DAPI stain (5 μg/ml, Sigma-Aldrich) for 10 minutes before the final washing steps. Coverslips were mounted on slides using Aqua Poly/Mount (Polysciences, Inc.) and subsequently analyzed on a Zeiss Axiovert microscope using a ×63 or ×100 objective, and micrographs collected as digital images on a SenSys cooled HCCD (Photometrics). Imaging of MURF-2 localization in mature myotubes was performed using a DeltaVision Deconvolution Model D-OL Olympus microscope with a ×100 objective using a Photometrics Series 300 CCD camera (Applied Precision). Images were processed for presentation using

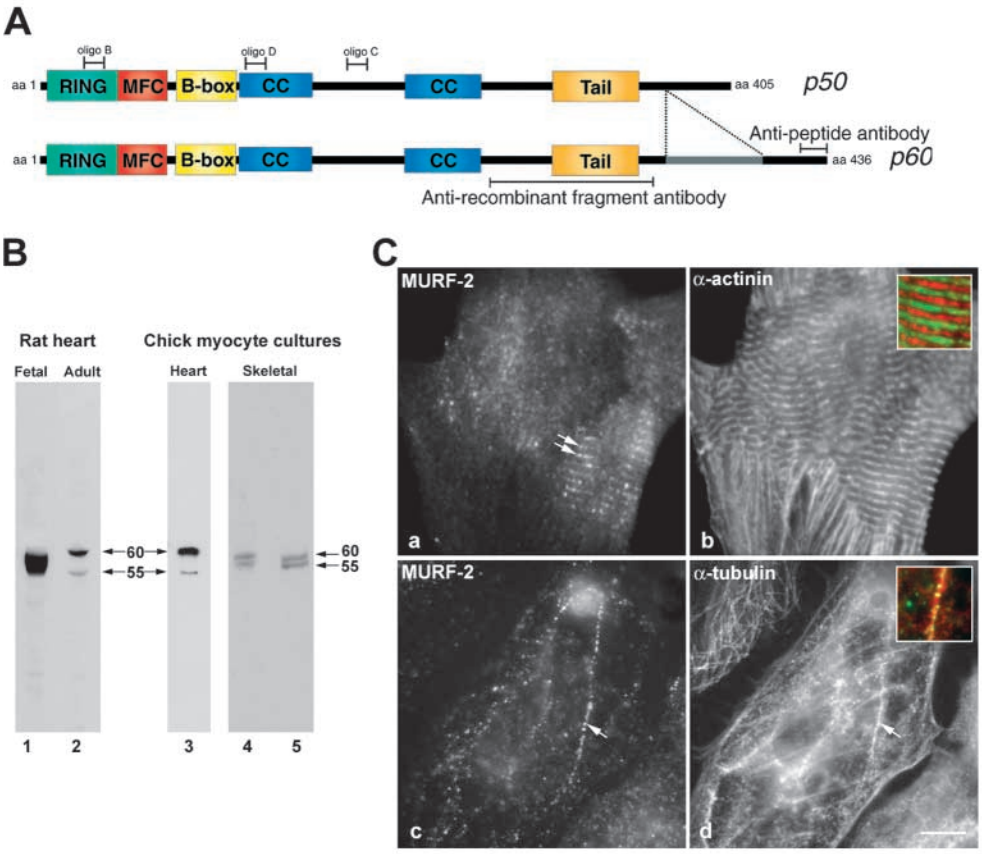

Fig. 1. Characterization of MURF-2 expression patterns in striated muscle. (A) MURF-2 contains a RING-finger domain (green), the MURF family conserved region (red), a B-box domain (yellow), two coiled-coil domains (blue), and an acidic tail (orange). Previous mRNA studies predicted four potential MURF-2 isoforms generated by differential splicing events within the 3′-region: p60 (full-length, lower schematic), p50 (upper schematic), a p27 isoform (missing the N-terminal region; not shown) and p60B (containing an alternate C-terminus generated by translation of alternative frames in the terminal exon; not shown). Two different antibodies were generated against the C-terminal region of mouse MURF-2. Antibodies against a synthetic peptide (the extreme 17 C-terminal residues) are predicted to recognize the full-length p60 MURF-2, as well as the p50 and p27 forms. Antibodies also were generated against an internal 83-residue, recombinant fragment containing the acidic tail domain (residues 278-365) shared by the p60, the p50, and the potential p60B splice forms. For further description of the potential p27 and p60B isoforms (see Pizon et al., 2002). Positions corresponding to the antisense oligonucleotides (B, C, and D) for chick MURF-2 also are indicated. (B) Anti-C-terminal MURF-2 antibodies recognize a broad band (55-60 kDa) in fetal rat heart lysates (lane 1) and two distinct bands (~55 and ~60 kDa) in adult rat heart lysates (lane 2), in primary cultures of embryonic chick cardiac myocytes (lane 3), and in primary cultures of chick skeletal myocytes (lane 4: myoblasts; lane 5: myotubes at day 3 of culture). (C) Immunofluorescence staining revealed that MURF-2 is detected diffusely in the cytoplasm, and at the M-line region of a portion of myofibrils (a: MURF-2, red; b: α-actinin, green; merged inset in b; double arrows point to striations). In the same culture, MURF-2 also was detected in a discontinuous, spotted pattern along a portion of microtubules in many chick cardiac myocytes (c: MURF-2, red; d: α-tubulin, green; merged inset in d; arrow points to tubulin staining). MURF-2 was not detected in fibroblasts (data not shown). Bar, 10 μm.

Photoshop 7.0 (Adobe) and statistical analyses were performed using Excel (Microsoft).

Results

Two developmentally regulated MURF-2 species are detected in muscle

MURF-2 mRNA studies revealed up to four potential isoforms generated by differential splicing events within the 3′-region of the gene: p60, p50 (Centner et al., 2001), p27 and p60B MURF-2 isoforms, the latter of which corresponds to an alternative C-terminus generated by translation of alternative frames in the terminal exon (Pizon et al., 2002). To investigate the expression of MURF-2 isoforms at the protein level further, polyclonal antibodies were generated against the acidic domain that is included in the predicted p60, p50, and p60B MURF-2 isoforms, and also the final 17 C-terminal residues, shared by p60, p50 and p27 (see Fig. 1A for schematic of MURF-2). Western blot analysis of rat heart muscle lysates using both affinity purified anti-peptide and anti-recombinant C-terminal MURF-2 antibodies detected two bands migrating at ~55 kDa and ~60 kDa, probably corresponding to the p50 and p60 MURF-2 isoforms (Fig. 1B). In adult rat muscle lysates, both bands were detected at longer exposures, although one broad band was consistently detected in fetal heart with short exposures (Fig. 1B, lanes 1 and 2). This broad band may correspond to high expression levels of the p50 and p60 MURF-2 isoforms in fetal heart, alternative fetal MURF-2 isoforms, and/or developmental differences in post-translational modifications. In primary cultures of chick cardiac and skeletal myocytes, we detected both bands throughout the culture period (Fig. 1B lane 3 for cardiac myocytes, lane 4 for myoblasts, lane 5 for myotubes at day 3 in culture). Thus, our western blot data are consistent with the co-expression of p50 and p60 MURF-2 isoforms, whereas an immunoreactive band corresponding to the p27 isoform was not detected in any of the muscle tissues or cell cultures investigated here. It remains to be determined whether the potential p60B protein is also co-expressed. In conclusion, p50 and p60 MURF-2 isoforms are expressed in both skeletal and heart muscle throughout development, but are down-regulated in adult muscle.

MURF-2 colocalizes with a portion of microtubules and the sarcomeric M-line region in cardiac myocytes

To determine the subcellular localization of MURF-2 in cardiac myocytes, we performed immunofluorescence staining and found that in all fetal rat and embryonic chick myocytes, MURF-2 was mainly observed in a diffuse pattern in the cytoplasm at varying intensities (Fig. 1C,a,c; data shown for chick). In addition, in around 50% of cardiomyocytes, MURF-2 was detected at the M-line region in some (20-30%) mature myofibrils (Fig. 1C,a,b): this region contains the titin binding site for MURF-1 (Centner et al., 2001; McElhinny et al., 2002). Additionally, MURF-2 colocalized in a spotted, discontinuous pattern along a portion of microtubules labeled with anti-α-tubulin antibodies in many (~70%) cardiac myocytes (Fig. 1C,c,d). These data are consistent with previous reports of both MURF-2 and MURF-3 associated with distinct populations of stable microtubules (Glu-MTs) in skeletal myocytes (Spencer et al., 2000; Pizon et al., 2002). It should also be noted that in around 10% of cardiac myocytes, MURF-2 was detected in rod, filamentous and 'squiggle'-like patterns of varying sizes, which did not colocalize with staining for any cytoskeletal components tested (data not shown). The significance of these patterns remains unclear. In addition, staining with either of our anti-MURF-2 antibodies (see above) yielded the same localization patterns. MURF-2 therefore exhibits multiple localizations in cardiac myocytes.

Knock-down of MURF-2 mRNA and protein levels disrupts stable microtubule populations

To gain insight into the function of MURF-2, we designed four different 16-mer antisense oligonucleotides to chicken MURF-2 expressed sequence tags (ESTs) and transfected them separately, and as a cocktail, into cultures of embryonic chick cardiomyocytes (see Fig. 1A). The cocktail, as well as three independent oligonucleotides, dramatically decreased levels of endogenous MURF-2 in a dose-dependent manner. (Less than 6 μg of total antisense oligonucleotide did not cause a significant knock-down of MURF-2 in the majority of myocytes, while greater than 12 μg was toxic. However, 10 μg resulted in significant MURF-2 knock-down without observable cellular toxicity, and this amount was used for all experiments.) The same phenotype was observed in fetal rat cardiac myocytes using three out of four oligonucleotides designed against the human MURF-2 sequences, and in chick myocytes using SiRNA oligos to the chick MURF-2 EST sequences (data not shown). Specifically, RT-PCR studies determined that MURF-2 mRNA transcript levels decreased in cultures treated with MURF-2 antisense oligonucleotides, but were unaffected in cells treated with control oligonucleotides (Fig. 2A, lanes 1, 2). GAPDH and MURF-3 levels appeared to be unchanged in antisense MURF-2 treated cultures, compared to controls (Fig. 2A, lanes 3-6). At the protein level, it is difficult to perform quantitative western blot analyses in antisense-treated primary cultures of myocytes for several reasons, including differences in the number of contaminating fibroblasts (which do not express MURF-2), which varies even among dishes from the same cultures (ranging from a total of 10-20%). However, by western blot analysis, we determined that both the levels of the 60 kDa and 55 kDa MURF-2 were consistently decreased by >50-70% in

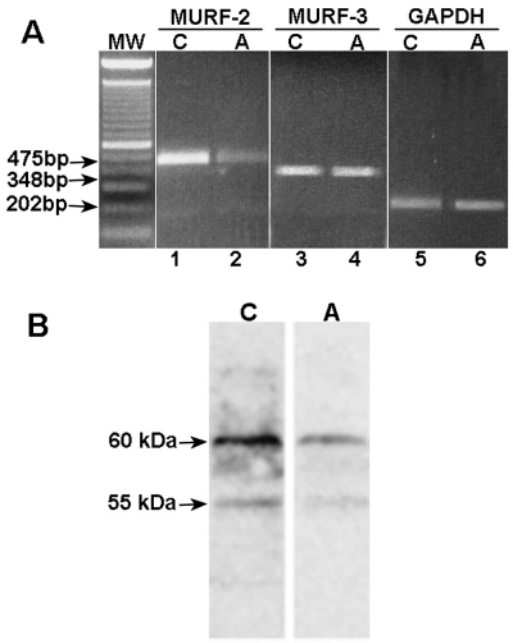

Fig. 2. (A) Antisense treatment of cardiac mycoytes knocks down MURF-2 mRNA and protein levels. Cardiac myocytes were treated with MURF-2 antisense or control oligonucleotides and RT-PCR was performed. MURF-2 mRNA transcript levels were significantly decreased in cultures treated with MURF-2 antisense oligonucleotides (lane 2) compared to control oligonucleotides (lane 1), although both GAPDH (lanes 5, 6) and MURF-3 (lanes 3, 4) mRNA transcript levels were unchanged. (B) Lysates of cardiac myocytes treated with control (C) or antisense (A) oligonucleotides were harvested 48 hours after treatment, protein assays were performed to ensure equal loading for SDS-PAGE, and transferred to nitrocellulose membranes. The strips were probed with anti-MURF-2 antibodies, revealing that both the 60 kDa and 55 kDa isoforms were significantly decreased in intensity (>50%) at the protein level in the antisense-treated lysates compared to control myocytes.

primary cultures of antisense-treated myocytes compared to controls within 48 hours after treatment (Fig. 2B). To confirm these observations on an individual cell basis, immunofluorescent staining for MURF-2 was performed, revealing that its intensity was diminished in more than 80% of cardiac myocytes within 24 hours of antisense treatment (data not shown), and barely detectable within 48 hours (Fig. 3A,f). MURF-2 levels began to return to pre-transfection levels within 72-96 hours (data not shown). In contrast, MURF-2 staining levels appeared unchanged in myocytes treated with control oligonucleotides at all timepoints (Fig. 3A,a and data not shown). Our results demonstrate that MURF-2 mRNA and protein levels were significantly reduced after antisense oligonucleotide treatment.

To examine the effects of MURF-2 knock-down on the cytoskeletal arrays with which it associates, we performed immunofluorescence studies to examine cardiac myocytes at the cellular level. Initially, co-staining antisense-treated myocytes with various antibodies that label microtubule populations yielded a striking phenotype. In more than 70% of MURF-2 antisense-treated myocytes, staining for α-tubulin (a marker for all microtubules) appeared less complex compared to control myocytes. Specifically, control myocytes contained

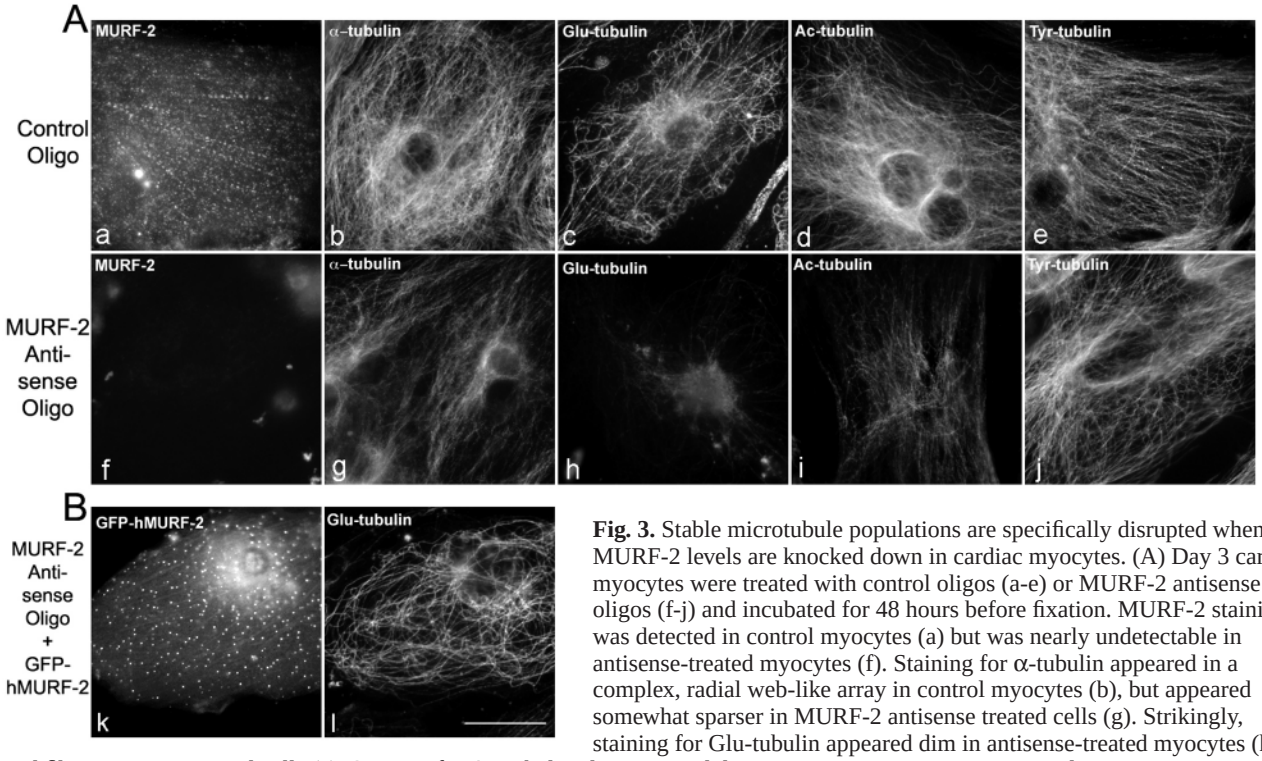

Fig. 3. Stable microtubule populations are specifically disrupted when MURF-2 levels are knocked down in cardiac myocytes. (A) Day 3 cardiac myocytes were treated with control oligos (a-e) or MURF-2 antisense oligos (f-j) and incubated for 48 hours before fixation. MURF-2 staining was detected in control myocytes (a) but was nearly undetectable in antisense-treated myocytes (f). Staining for α-tubulin appeared in a complex, radial web-like array in control myocytes (b), but appeared somewhat sparser in MURF-2 antisense treated cells (g). Strikingly, staining for Glu-tubulin appeared dim in antisense-treated myocytes (h), but bright and filamentous in control cells (c). Staining for Ac-tubulin also appeared dimmer in MURF-2 antisense treated myocytes compared to control cells (d,i). Finally, staining for the dynamic Tyr-MT populations did not appear to differ between control (e) and MURF-2 antisense treated cells (j). (B) Human GFP-MURF-2 expression rescues Glu-MTs in antisense-treated chick myocytes. Chick cardiac myocytes co-transfected with MURF-2 antisense oligos and human GFP-MURF-2 also were stained for Glu-tubulin. Myocytes expressing GFP-hMURF-2 (k), often detected in aggregates in the cytoplasm, contained bright, complex arrays of Glu-MTs (l) compared to antisense-treated myocytes not expressing GFP-h-MURF-2 (Fig. 3A,h). Bar, 10 μm.

microtubules in dense, complex web-like radial arrays or thick, parallel arrays that coursed throughout their cytoplasm, whereas in antisense-treated myocytes, the microtubules appeared less three-dimensional as observed by changing focal planes (Fig. 3A,b,g).

To investigate this phenotype further, we used a panel of well-characterized antibodies that label distinct populations of microtubules. The vast majority of myocytes treated with MURF-2 antisense oligonucleotides exhibited a dramatic disruption of the stable microtubule array; that is, staining for Glu-MTs consistently appeared dimmer compared with the bright, complex patterns of arrays observed in control myocytes (Fig. 3A,c,h). In striking contrast, Glu-MTs appeared unaffected in all antisense-treated fibroblasts that contaminated the cultures, indicating that the phenotype was not due to general toxic effects from the antisense oligonucleotides (data not shown). To confirm that this phenotype was due specifically to a decrease in MURF-2 levels, we co-transfected chick cardiac myocytes with MURF-2 antisense oligonucleotides and a construct encoding the 60-kDa isoform of human MURF-2-GFP for rescue experiments. The chick MURF-2 antisense sequences were not significantly complementary to the human MURF-2 cDNA sequence (i.e., there were $\geqslant$3 nucelotide differences/16-mer oligo) and did not appear to reduce human GFP-MURF-2 expression. It should be noted that overexpression of MURF-GFP fusion proteins resulted in aggregates of varying size throughout the cytoplasm, probably due to their homo-oligomerization (Spencer et al., 2000; McElhinny et al., 2002) (Fig. 3B,k). The majority of antisense-treated myocytes expressing human MURF-2-GFP fusion protein contained bright Glu-tubulin staining, mainly in complex radial patterns (Fig. 3B,l), in contrast to antisense treated myocytes not expressing human MURF-2-GFP on the same coverslips (Fig. 3A,h). These data indicate that human MURF-2 rescues Glu-MT integrity in cardiac myocytes with reduced levels of endogenous chick MURF-2.

Additionally, we found that the acetylated microtubule arrays (Ac-MTs), which largely overlap with Glu-MTs, also appeared sparser in around 60% MURF-2 antisense-treated myocytes compared to controls, although they did not appear disrupted to the same extent as the Glu-MTs in antisense-treated myocytes (Fig. 3A,d,i). Therefore, it is possible that the effect on the Ac-MT in the MURF-2 antisense-treated myocytes was secondary to the disruption of the Glu-MTs. Finally, in contrast to the stable microtubule populations, the integrity of the dynamic Tyr-MT appeared unaffected by a decrease in MURF-2 levels in all cardiac myocytes examined (Fig. 3A,e,j). The loss of Glu-MT and Ac-MT integrity, combined with a lack of disruption observed for the Tyr-MT populations, is likely to be responsible for α-tubulin staining appearing only partially affected by MURF-2 knock-down (Fig. 3A,b,g). In conclusion, these data indicate that MURF-2 expression is required for the integrity of stable (Glu-MT and Ac-MT), but not dynamic (Tyr-MT), microtubule arrays in cardiac myocytes.

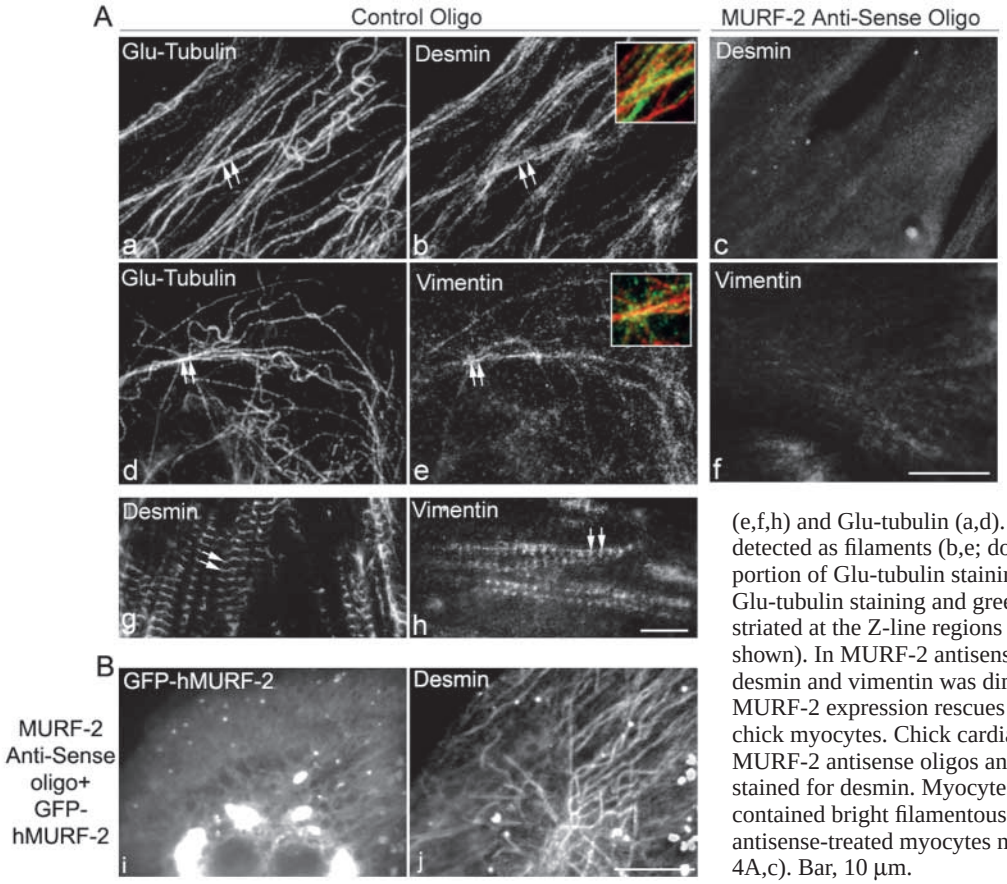

Fig. 4. Staining for the intermediate filament proteins, desmin and vimentin, is also perturbed in MURF-2 antisense-treated cardiac myocytes. (A) Chick cardiac myocytes treated with control (a,b,d,e,g,h) or MURF-2 antisense oligonucleotides (c,f) were co-stained for desmin (b,c,g), vimentin (e,f,h) and Glu-tubulin (a,d). Desmin and vimentin staining was detected as filaments (b,e; double arrows) that colocalized with a portion of Glu-tubulin staining (a,d; merged insets in b, e; red is Glu-tubulin staining and green is desmin or vimentin), as well as striated at the Z-line regions (g,h) and at cell junctions (data not shown). In MURF-2 antisense treated myocytes, staining for desmin and vimentin was dim and diffuse (c,f). (B) Human GFP-MURF-2 expression rescues desmin staining in antisense-treated chick myocytes. Chick cardiac myocytes co-transfected with MURF-2 antisense oligos and human GFP-MURF-2 also were stained for desmin. Myocytes expressing GFP-hMURF-2 (i) contained bright filamentous desmin staining (j), compared to antisense-treated myocytes not expressing GFP-h-MURF-2 (Fig. 4A,c). Bar, 10 μm.

Proper MURF-2 levels also are required for desmin and vimentin structure in cardiac myocytes

As Glu-MTs are required for the localization and maintenance of intermediate filament proteins in fibroblasts (Gyoeva and Gelfand, 1991; Gurland and Gundersen, 1995), we co-stained myocytes for Glu-tubulin and the intermediate filament proteins, desmin and vimentin, to determine whether these arrays may be linked in muscle. As previously reported, desmin is organized in different patterns in adult and embryonic cardiac myocytes (Nag et al., 1986; Nag and Huffaker, 1998). In our cultures, desmin was detected as a filamentous network and in ribbon-like strands in many myocytes; in these cells, a portion of desmin staining co-localized with Glu-tubulin staining (Fig. 4A,a,b). Similarly, Glu-MTs colocalized with a portion of vimentin filaments in cardiac myocytes (Fig. 4A,d,e). Desmin and vimentin were also detected in many cardiac myocytes in regular, striated patterns at the Z-lines of myofibrils (Fig. 4A,g,h), and also at cell junctions (data not shown); neither pattern colocalized with Glu-MTs (data not shown). Strikingly, desmin and vimentin staining was diffuse and dim in the majority of cardiac myocytes treated with MURF-2 antisense oligonucleotides (Fig. 4A,c,f). These data were confirmed by staining chick myocytes with two other independent desmin antibodies (data not shown). Furthermore, the loss of desmin filament integrity was rescued upon co-transfection with the human MURF-2-GFP construct in cardiac myocytes (Fig. 4B,i,j). Considered together, these data suggest that MURF-2 expression is also required for intermediate filament structure in cardiac myocytes.

Knock-down of MURF-2 in cardiac myocytes also perturbs the M-line region of sarcomeres and affects contractile activity

As MURF-2 also localizes to the M-line region (Fig. 2B), we investigated the effect of MURF-2 knock-down on the integrity of myofibril components. Approximately 80% of MURF-2 antisense-treated myocytes exhibited disrupted staining for M-line components, including the M-line region of titin (using both anti-A168-170 and titin AB5 antibodies; data shown for AB5, Fig. 5A,l), and myomesin (Fig. 5A,k), in comparison to control myocytes that displayed regular striations typical for these proteins (Fig. 5A,h,i). In contrast, the Z-line marker, α-actinin, the Z-line peripheral region of titin (T11), and the thick filament component, myosin, all appeared in regular, striated patterns in myocytes treated with MURF-2 antisense oligonucleotides (Fig. 5A,e,f,j compared with b,c,g). Thin filaments also appeared in a typical striated pattern in antisense-treated myocytes (data not shown). The disruption of sarcomeric M-line integrity also could be rescued upon co-transfection with human MURF-2-GFP in the majority of co-transfected cardiac myocytes (Fig. 5B,m,n).

Finally, the contractile activity of the cardiac myocytes was affected with reduced levels of MURF-2. Specifically, ~20% of the cardiac myocytes in the antisense-treated myocytes were observed to beat within 24-48 hours of treatment, compared to more than 60% of control myocytes. The MURF-2 antisense-treated myocytes that did contract appeared to do so faster than the control myocytes within 48 hours of treatment (data not shown). Additionally, it should be noted that knock-down of

MURF-2 was maintained for about 4 days in culture by spiking the cells with lipid and antisense oligonucleotides within 48 hours of the initial treatment (data not shown). It was determined that the disrupted microtubules, intermediate filament proteins, M-lines, and loss of contractile activity (as described above) persisted throughout the entire culture period, yet no disruption of other cytoskeletal components was observed (data not shown). This indicates that MURF-2 is important for microtubule, intermediate filament, M-line structure and contractile activity in cardiac myocytes.

MURF-2 colocalizes with a portion of microtubules and then associates with assembling myofibrils in differentiating chick skeletal myocytes

We performed antisense studies in primary cultures of chick skeletal myotubes as a complementary model system to the cardiac myocytes. Myoblasts are derived from skeletal muscle satellite cells, making it feasible to study differentiation and de novo myofibrillogenesis (e.g. Gregorio and Antin, 2000). In addition, regulated microtubule dynamics are known to be critical for skeletal muscle differentiation, morphology and myofibrillogenesis (Antin et al., 1981; Gundersen et al., 1989; Mangan and Olmsted, 1996). As in cardiac myocytes, the majority of MURF-2 staining appeared diffuse in the cytoplasm throughout the culture period (Fig. 6a,c,e). In ~60% of elongating myoblasts and ~40% of early myotubes, a portion of MURF-2 colocalized with α-tubulin staining (Fig. 6a,b). However, at intermediate and later stages of differentiation, MURF-2 staining was not colocalized with microtubules (data not shown). Specifically, at intermediate stages of myofibrillogenesis, MURF-2 staining was still detected diffusely in the cytoplasm but also at the M-line region in some myofibrils (Fig. 6c,d). In fact, MURF-2 staining was detected at the M-line region much less frequently in skeletal myotubes compared with cardiac myocytes (<5% of myofibrils in skeletal myotubes compared to 20-30% of myofibrils in cardiac myocytes). Additionally, late in myofibrillogenesis, MURF-2 staining remained diffuse in the cytoplasm and associated along the length of assembling and more mature myofibrils (Fig. 6e,f).

Knock-down of MURF-2 in chick skeletal myoblasts delays fusion events and myofibrillogenesis

We treated skeletal myoblasts with MURF-2 antisense oligonucleotides or control oligonucleotides immediately prior to plating. Myoblasts treated with MURF-2 antisense oligonucleotides were elongated within 24 hours, but did not fuse to the same extent as control myoblasts (Fig. 7a,b). After 48 hours, the MURF-2 antisense-treated cells began to fuse, but still lagged behind the control myotubes (Fig. 7c,d). By 72 hours after treatment, the antisense-treated myotubes appeared significantly thinner and less branched than the control myotubes (Fig. 7e,f). Furthermore, although control myotubes were often twitching at this time, antisense treated myotubes were not observed to twitch until ~96 hours after treatment, when they were morphologically indistinguishable from controls (Fig. 7g,h).

To examine this phenotype more thoroughly, we fixed and

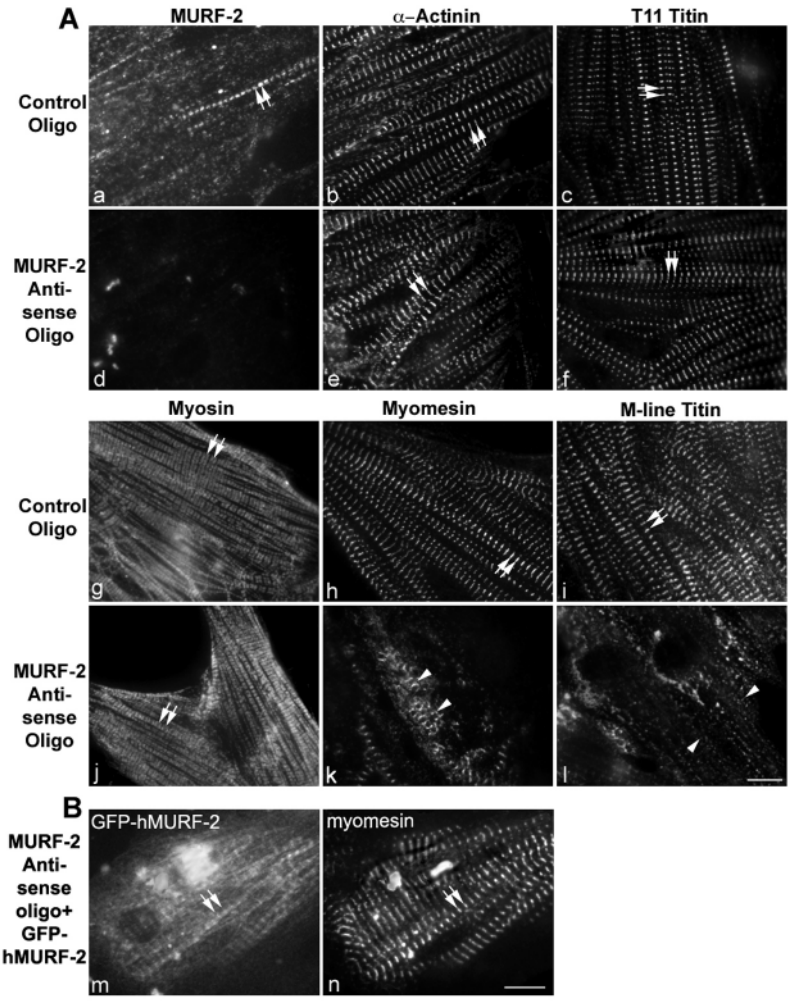

Fig. 5. Knock-down of MURF-2 levels specifically disrupts M-line region components of myofibrils, but not Z-lines or thick filament components. Chick cardiac myocytes were treated with antisense oligonucleotides to MURF-2 or control oligonucleotides, fixed 48 hours later, and stained for various sarcomeric components. Control myocytes exhibited bright staining for MURF-2 and staining for α-actinin, the peripheral Z-line region of titin (T11 epitope), myosin, and the M-line components myomesin and the M-line region of titin (AB5) in regular, striated patterns (a-c, g-i). Myocytes that had knocked-down levels of MURF-2 (d) exhibited staining for α-actinin, titin T11, and myosin in regular, striated patterns (e,f,j). However, in ~80% of the antisense-treated myocytes, staining for the M-line components myomesin and the C-terminal region of titin was strikingly disrupted (k,l). Double arrows point to regular striations and single arrowheads point to disrupted myofibrils. (B) Human GFP-MURF-2 expression rescues myomesin staining in antisense-treated chick myocytes. Chick cardiac myocytes co-transfected with MURF-2 antisense oligos and human GFP-MURF-2 were co-stained for myomesin. Myocytes expressing GFP-hMURF-2 (m) contained regular, striated myomesin staining (n), compared to antisense-treated myocytes not expressing GFP-h-MURF-2 (k). Bar, 10 μm.

stained the cells at various times in culture. Within 24 hours of treatment, MURF-2 staining was dim in the majority of myotubes treated with antisense oligonucleotides, suggesting that MURF-2 levels were significantly lowered; in these myocytes, staining for both α-tubulin and desmin was dim compared to controls (Fig. 8A,e,f,h). In contrast, staining for both α-actinin and myosin were at comparable intensities with control cells (data not shown). Furthermore, the α-tubulin and desmin staining in the antisense-treated myotubes also was dimmer than in control myocytes observed from earlier stages in culture (data not shown), indicating that the phenotype was not simply due to developmental delay upon MURF-2 knock-down. The antisense-treated myotubes were thin, and staining with DAPI revealed that they contained a mean of only ~6 nuclei/myotube, significantly fewer than control myotubes with ~16 nuclei/myotube (Fig. 8A,c,g; 8B). Myoblasts co-transfected with both antisense oligonucleotides and the human MURF-2-GFP construct were able to fuse similar to control myoblasts (mean of ~12.5 compared to ~14 nuclei/myotube, respectively), indicating that this phenotype was rescued by exogenous expression of human MURF-2 (Fig. 8C).

Within 48 hours of antisense treatment, the MURF-2 staining in treated myotubes was comparable in intensity to that in control myotubes (Fig. 8A,i,m), indicating that MURF-2 levels were recovering from the antisense knock-down. Although the antisense-treated myotubes remained thinner and smaller than the controls, α-tubulin staining appeared in regular, parallel array as in the controls, and desmin also appeared bright and normally distributed throughout the myotubes (Fig. 8A,j,l,n,p). Within 96 hours both populations of myotubes appeared similar in size and morphology (see Fig. 7). Thus, the antisense-treated myotubes appeared to recover after MURF-2 levels appeared at normal intensities. Unfortunately, differentiated myotubes

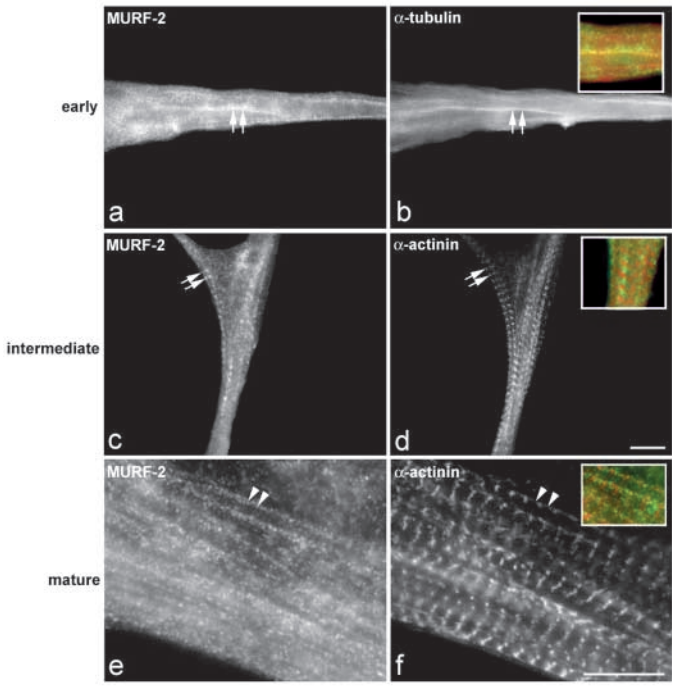

Fig. 6. MURF-2 colocalizes with a portion of microtubules and with assembling myofibrils in primary cultures of skeletal myocytes. Myofibrillogenesis in skeletal myogenic cells was analyzed by costaining myotubes for α-actinin (d,f and data not shown). MURF-2 staining was mainly diffuse in the cytoplasm throughout the culture period (a,c,e). In addition, some MURF-2 staining was detected colocalized with α-tubulin staining early in culture (a,b; merged inset in b; red is MURF-2 staining and green is tubulin; double arrows point to colocalization). Later during myofibrillogenesis, MURF-2 staining was detected at the M-line region, although in relatively few myofibrils (c,d; merged image in d; MURF-2 staining in red, α-actinin staining is green; double arrows point to myofibrils). In mature myotubes, MURF-2 staining also could be detected along the length of some myofibrils (e,f; double arrowheads). Bar, 10 μm.

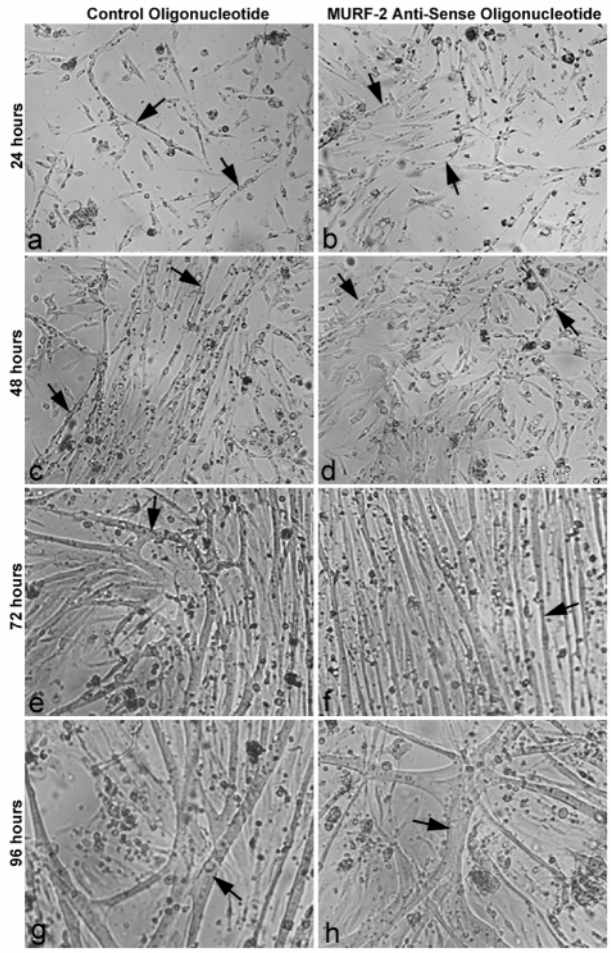

Fig. 7. Treatment of skeletal myoblasts with MURF-2 antisense oligonucleotides delays fusion events. Primary cultures of chick myoblasts were treated with control or MURF-2 antisense oligonucleotides and observed by phase microscopy at different stages of differentiation. Within 24 hours of treatment, control myoblasts were elongating, aligning, and beginning to fuse (a, arrows). In contrast, myoblasts treated with MURF-2 antisense oligonucleotides were elongated, but were not fusing (b, arrows). Within 48 hours of treatment, control myotubes were fusing extensively, although MURF-2 antisense-treated cells appeared only to be beginning to fuse (c,d, arrows). Control myotubes were thick and branched within 72 hours of treatment (e, arrow) and were often twitching, although antisense-treated myotubes appeared thinner, much less branched (f, arrow), and were not observed to twitch. Within 96 hours of treatment, control and antisense-treated myotubes appeared indistinguishable by light microscopy (g,h, arrows), and both populations of myotubes were observed to twitch.

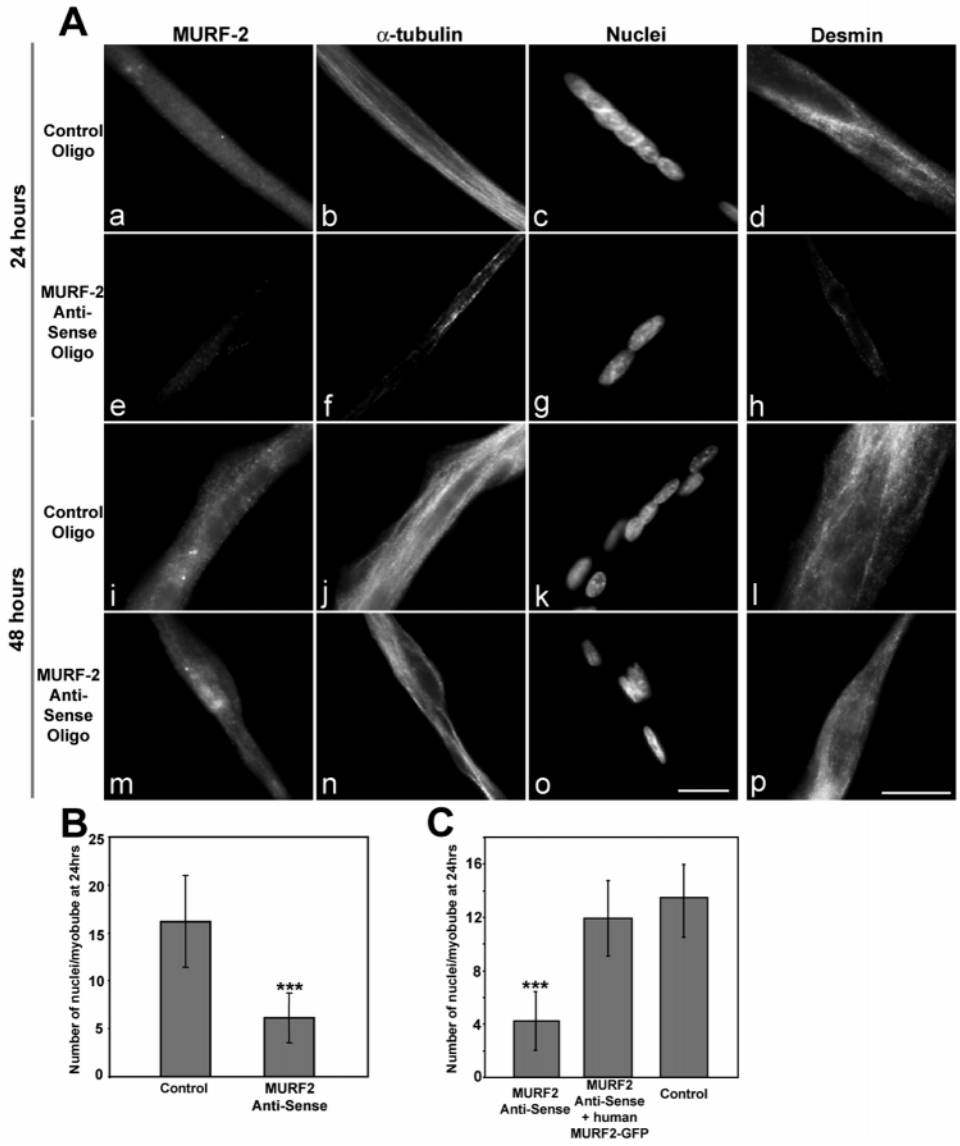

Fig. 8. Knock-down of MURF-2 levels in chick skeletal myoblasts perturbs α-tubulin and desmin staining and significantly inhibits fusion. (A) Skeletal myoblasts were treated with antisense or control oligonucleotides and fixed at 24 or 48 hours. The cells were stained with antibodies to α-tubulin (b,f,j,n) and with DAPI (c,g,k,o) to quantify the number of nuclei/myotube as a measure of fusion. Within 24 hours of treatment, thick control myotubes contained diffuse MURF-2 staining, bright filamentous microtubules parallel to the longitudinal axis, and bright, diffuse desmin staining (a,b,d). Control myotubes also had a mean of ~16 nuclei (c,B) (note: the myotube in c also had nuclei outside the field of view). In contrast, antisense-treated myotubes were strikingly thin, had low levels of MURF-2 staining (e), low α-tubulin and desmin staining (f,h) and significantly fewer nuclei (g,B). Within 48 hours of treatment, MURF-2 levels were comparable in antisense-treated myotubes (m) and control myotubes (i), and α-tubulin staining in both populations of myotubes appeared in bright filaments (j,n). Desmin staining appeared bright and diffuse in both populations of myotubes (l,p). However, the MURF-2 antisense treated myotubes remained thinner and qualitatively contained fewer nuclei/myotube compared to controls (k,o). Note that the large number of overlapping nuclei/myotube could not be quantified accurately at 48 hours in control myotubes. Bar, 10 μm. (C) Human GFP-MURF-2 expression rescues fusion events in antisense-treated chick skeletal myotubes. Chick skeletal myoblasts were co-transfected with MURF-2 antisense oligos and human GFP-MURF-2, fixed 24 hours after treatment, and stained with DAPI to quantify the number of nuclei per myotube. Myotubes expressing GFP-hMURF-2 (*n*=15 from two different cultures) contained similar numbers of nuclei/myotube compared to myotubes treated with control oligonucleotides; both populations contained significantly greater numbers of nuclei/myotube compared with antisense-treated myotubes not expressing human MURF-2-GFP.

are very difficult to transfect (reviewed in Antolik et al., 2003), and as a result we were unable to knock-down MURF-2 levels at later stages of differentiation, nor maintain the initial knock-down.

Finally, we also determined whether myofibrillogenesis was affected in the MURF-2 antisense-treated myotubes. Within 48 hours, the antisense-treated myotubes contained the sarcomeric components α-actinin, myosin, and the C-terminal region of titin in filamentous and diffuse patterns (Fig. 9d-f), yet the thick, branched control myotubes were assembling these components into striated patterns (Fig. 9a-c). Within 72-96 hours, both control and MURF-2 antisense-treated myotubes contained all sarcomeric components examined in normal striated patterns (Fig. 9g-l; data shown for 72 hours). These studies indicate that knock-down of MURF-2 levels during the myoblast stage delayed myofibrillogenesis, but these events occurred after MURF-2 staining appeared at normal intensities (see Fig. 8). In conclusion, MURF-2 is involved in fusion events, the integrity of microtubules and desmin, proper contractile activity and myofibrillogenesis.

Discussion

MURF-2 has been the least-characterized member of the muscle RING finger protein family: three structurally related molecules quickly emerging as key players in striated muscle functions. We designed these studies to decipher the physiological roles of MURF-2, the only family member that is developmentally down-regulated. We found that MURF-2 has multiple roles in cardiac and skeletal myocytes. Consequently, important questions now arise concerning its properties and mechanisms of action.

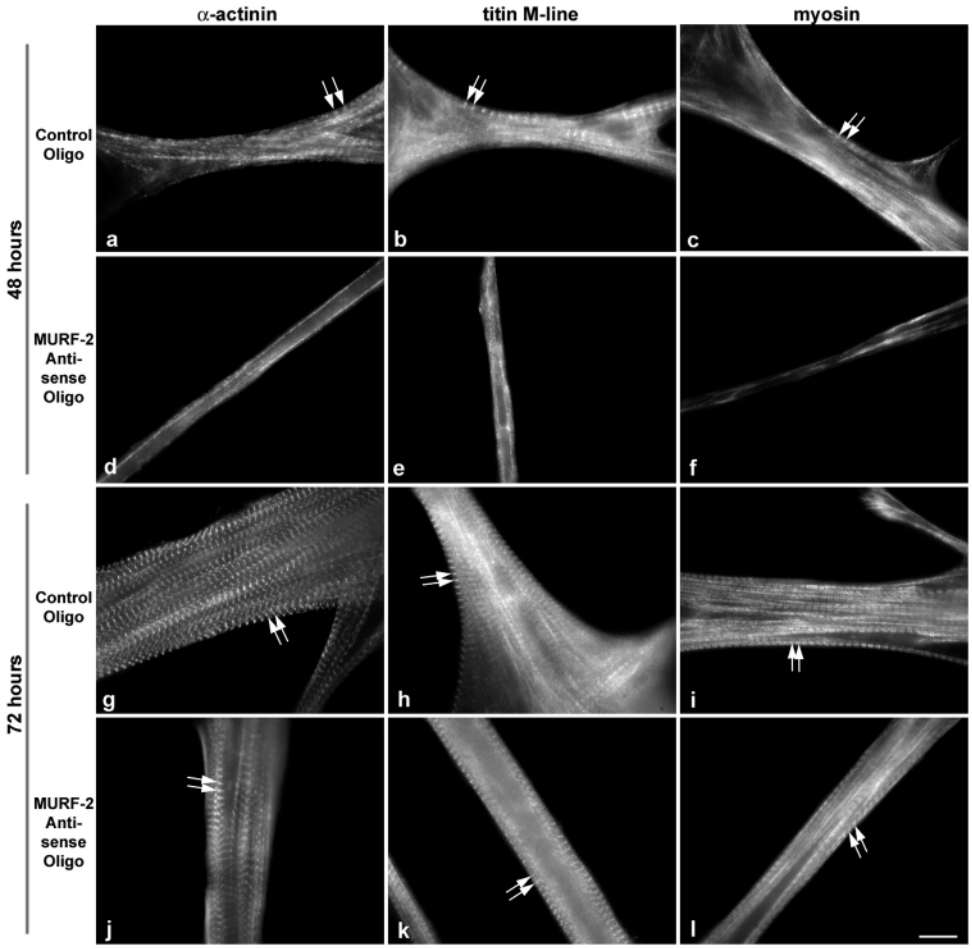

Fig. 9. Myofibrillogenesis is delayed in chick skeletal myotubes after treatment with MURF-2 antisense oligonucleotides. Control or MURF-2 antisense-treated myotubes were fixed after 48 or 72 hours of treatment and stained for various sarcomeric components to analyze myofibril assembly. Within 48 hours of treatment, the majority of control myotubes were beginning to assemble α-actinin, the M-line region of titin (A168-170), and myosin into regular, striated patterns (a,b,c, double arrows). In contrast, myotubes treated with MURF-2 antisense oligonucleotides were thin and exhibited no myofibril components in striated patterns (d,e,f). Within 72 hours of treatment, both control and MURF-2 antisense treated myotubes contained α-actinin, the M-line region of titin, and myosin in regular, striated patterns (g-l, double arrows), although the antisense-treated myotubes still appeared thinner than controls (j-l). Bar,10 μm.

MURF-2 and microtubules

First, our studies reveal that MURF-2 expression is specifically required for the integrity of stable Glu-MTs and Ac-MTs, but not the dynamic Tyr-MTs. These data are particularly intriguing given that MURF-2 colocalizes with only a portion of cardiac microtubules and appears to be only transiently associated with skeletal myocyte Glu-MTs early in differentiation (see also Pizon et al., 2002): therefore, it does not appear to be an integral microtubule component. We speculate that MURF-2 may interact with microtubules via hetero-oligomerization with MURF-3, a protein that associates with Glu-MTs throughout development (Centner et al., 2001; Spencer et al., 2000). Perhaps MURF-2 plays an accessory role in microtubule stabilization, whereas MURF-3 acts as the primary stabilizer. In this regard, the molecular mechanisms responsible for regulating Glu-MT stability have remained elusive. Previous studies determined that detyrosination alone is insufficient for microtubule stabilization (Khawaja et al., 1988; Webster et al., 1990), and that Glu-MTs are bound at the plus ends by unidentified ATP-sensitive capping complexes (Infante et al., 2000). The molecular identities of microtubule associated proteins (MAPs) specific for stabilization of Glu-MT filaments are unknown and therefore it is an exciting possibility that MURF-2 and MURF-3 fulfill this role in muscle. This idea is particularly intriguing given that stable microtubule arrays are required for normal muscle development and function (e.g. Gundersen et al., 1989). Alternatively, MURF-2 and/or MURF-3 may collaborate with other molecules: for instance, the muscle-specific MAP4 is required for skeletal muscle morphology and myofibrillogenesis (Mangan and Olmsted, 1996). Further studies, including analyses of MURF-2 and MURF-3 null models will provide insight into these complex issues.

It also is important to note that the Ac-MT arrays were disrupted in cardiac myocytes upon loss of MURF-2. Relatively little is known of the Ac-MT population, although their levels are known to increase after the Glu-MT network has been established and myoblasts have fused (Gundersen et al., 1989). Furthermore, acetylation and detyrosination occur in distinct, but overlapping, microtubule populations (Schulze et al., 1987; Bulinski et al., 1988; Chang et al., 2002). Whether MURF-2 levels affect entire stable arrays of muscle microtubules (which are probably comprised of several distinct, post-translationally modified populations in addition to Glu- and Ac-MTs) remains to be determined.

MURF-2 and intermediate filaments

A decrease in MURF-2 levels also perturbed the structure of the intermediate filament proteins, vimentin and desmin. It has been reported that in fibroblasts and some cell lines, Glu-MTs localize and stabilize intermediate filaments, yet intermediate filaments are not required for Glu-MT stability (Gyoeva and Gelfand, 1991; Gurland and Gundersen, 1995; Liao and

Gundersen, 1998; Kreitzer et al., 1999). Our data suggest that Glu-MTs serve a similar function in striated muscle; that is, disruption of Glu-MTs upon knock-down of MURF-2 may have secondarily disrupted vimentin and desmin structure. This mechanism does not account, however, for desmin and vimentin localized in striated patterns and at cell junctions, which do not colocalize with Glu-MTs. Insight into these caveats requires further biochemical and functional studies focussed on muscle intermediate filaments and microtubule populations. Additionally, studies are needed to determine whether MURF-2 mediates the interaction between desmin, vimentin and Glu-MTs, as well as whether other intermediate filament proteins expressed in striated muscle also are affected upon MURF-2 knock-down.

MURF-2, the sarcomeric M-line region, and myofibrillogenesis

Knock-down of MURF-2 in cardiac myocytes dramatically disrupted staining for myofibrillar M-line components, including myomesin and the C-terminal region of titin. Strikingly, however, the integrity of the N-terminal region of titin appeared unaffected, indicating that the giant molecule was specifically disrupted at the M-line region. Furthermore, the Z-line marker α-actinin, the thick filaments, and the thin filaments were undisrupted by a loss of MURF-2. Several mechanisms responsible for this phenomenon are possible. First, MURF-2 may directly associate with titin to regulate M-line assembly during myofibrillogenesis (Pizon et al., 2002). Another possible model is that MURF-2 hetero-oligomerizes with MURF-1 to aid in M-line assembly events. This model is supported by observations that MURF-1 and MURF-2 hetero-oligomerize in vitro, and GFP-MURF-1 and MURF-2 colocalize at the M-line region of titin in transfected cardiac myocytes (A. S. McElhinny, S. Labeit, and C. C Gregorio, unpublished data). Perhaps the stoichiometry of MURF-1 and MURF-2 oligomers governs events at the M-line during its assembly and/or turnover during muscle development. Later in development when MURF-2 is down-regulated, MURF-1 may be recruited as the primary molecule to regulate titin M-line structure in response to stress and/or atrophy signals (for example, involving GMEB-1 activation). It is tempting to speculate that these events involve regulation via the kinase domain of titin (Centner et al., 2001).

It also should be noted that several groups hypothesize that microtubules serve as dynamic scaffolds for assembling myofibrils (Antin et al., 1981; Toyama et al., 1982). Our data reveal that disruption of stable microtubules in embryonic cardiac myocytes upon MURF-2 knock-down specifically disrupts M-line integrity in myofibrils. Therefore, it appears that microtubules have links to the sarcomeric M-line region, probably via MURF-2 and the titin kinase region.

Finally, our investigations into the function of MURF-2 during de novo myofibrillogenesis in skeletal myocytes revealed that its proper expression is essential for myoblast fusion events. Thus, it appears that both MURF-2 and MURF-3 are required for muscle differentiation (this study) (Spencer et al., 2000), although their mechanisms of action remain unclear. Since both MURFs appear to associate with Glu-MTs, the population of microtubules established around the time of fusion and required for fusion events (Gundersen et al., 1989; Chang et al., 2002), we favor a model in which MURF-2 stabilizes Glu-MTs early in skeletal muscle differentiation to permit fusion and subsequent myofibrillogenesis to occur. However, we cannot rule out the possibility that MURF-2 is a necessary component of pathways involved in differentiation events that occur upstream of the establishment and/or rearrangement of cytoskeletal arrays in muscle development. Whether MURF-2 plays signaling roles in myocytes, either as a primary function and/or in addition to structural functions, remains an exciting question for the future.

MURF-2, contractile activity, and disease

Intriguingly, the beating rate of neonatal cardiomyocytes is regulated by the stable microtubule subset (Webster and Patrick, 2000), and treatment of cardiac myocytes with nocodazole increases contractile activity (Rothen-Rutishauser et al., 1998). Therefore, microtubules appear to function as negative regulators of muscle contraction (Webster, 2000). In agreement with this idea, cardiac hypertrophy and failure correlate with increases in Glu-tubulin and MAP4 levels (Sato et al., 1997; Belmadani et al., 2002; Takahashi et al., 2003). It is an exciting possibility, then, that mis-regulation of MURF-2 (and MURF-3) levels also could contribute to human contractile dysfunction. Consistent with this idea, we found that MURF-2 knock-down affected normal contractile activity in both skeletal and cardiac myocytes: in many myocytes, contractile activity was not observed, although in some myocytes the beating rate was increased.

In conclusion, it is becoming apparent that the MURF family members play important roles in the development and maintenance of striated muscle. Intriguingly, MURF-2 appears to be the only MURF family member with links to intermediate filaments, microtubules, and the M-line region of the sarcomere. In this regard, we propose that MURF-2 acts as a molecule shuttle to link these cytoskeletal arrays during muscle development, and that at least some of its functions may be regulated by titin-based signaling events. However, it is also possible that MURF-2 may affect the expression or activity of other, unidentified molecules important for proper cytoskeletal interactions and function in muscle, or it may also be an integral player in differentiation pathways critical for the establishment of proper cytoskeletal arrays. The multiple roles of MURF-2 in normal muscle differentiation as proposed here merit further investigation.

The authors gratefully acknowledge Ryan Mudry for expert assistance with microscopy and assembling the figures. We thank Catherine Schwach, Adam Geach and Matthew Smith (University of Arizona) for excellent technical assistance. We are indebted to Ray Runyan (University of Arizona) and J. Chlöe Bulinski (Columbia University) for helpful discussions. This study was funded by grants from the American Heart Association (0120586Z) to A.S.M., NSF (DBI 9912036) to C.N.P., Deutsche Forschungsgemeinschaft (La668/7-1) to S.L., and NIH (HL63926) and (HL03985) to C.C.G.

References

Almenar-Queralt, A., Gregorio, C. C. and Fowler, V. M. (1999). Tropomodulin assembles early in myofibrillogenesis in chick skeletal muscle: evidence that thin filaments rearrange to form striated myofibrils. *J. Cell Sci.* **112**, 1111-1123.

Antin, P. B., Forry-Schaudies, S., Friedman, T. M., Tapscott, S. J. and

Holtzer, H. (1981). Taxol induces postmitotic myoblasts to assemble interdigitating microtubule-myosin arrays that exclude actin filaments. *J. Cell Biol.* **90**, 300-308.

Antolik, C., de Deyne, P. G. and Bloch, R. J. (2003). Biolistic transfection of cultured myotubes. *Sci. STKE* **2003**, pl11.

Balogh, J., Merisckay, M., Li, Z., Paulin, D. and Arner, A. (2002). Hearts from mice lacking desmin have a myopathy with impaired active force generation and unaltered wall compliance. *Cardiovasc. Res.* **53**, 439-450.

Bang, M. L., Mudry, R. E., McElhinny, A. S., Trombitas, K., Geach, A. J., Yamasaki, R., Sorimachi, H., Granzier, H., Gregorio, C. C. and Labeit, S. (2001). Myopalladin, a novel 145-kilodalton sarcomeric protein with multiple roles in Z-disc and I-band protein assemblies. *J. Cell Biol.* **153**, 413-427.

Belmadani, S., Pous, C., Ventura-Clapier, R., Fischmeister, R. and Mery, P. F. (2002). Post-translational modifications of cardiac tubulin during chronic heart failure in the rat. *Mol. Cell. Biochem.* **237**, 39-46.

Boardman, P. E., Sanz-Ezquerro, J., Overton, I. M., Burt, D. W., Bosch, E., Fong, W. T., Tickle, C., Brown, W. R., Wilson, S. A. and Hubbard, S. J. (2002). A comprehensive collection of chicken cDNAs. *Curr. Biol.* **12**, 1965-1969.

Bodine, S. C., Latres, E., Baumhueter, S., Lai, V. K., Nunez, L., Clarke, B. A., Poueymirou, W. T., Panaro, F. J., Na, E., Dharmarajan, K. et al. (2001). Identification of ubiquitin ligases required for skeletal muscle atrophy. *Science* **294**, 1704-1708.

Boudriau, S., Vincent, M., Cote, C. H. and Rogers, P. A. (1993). Cytoskeletal structure of skeletal muscle: identification of an intricate exosarcomeric microtubule lattice in slow- and fast-twitch muscle fibers. *J. Histochem. Cytochem.* **41**, 1013-1021.

Bulinski, J. C., Richards, J. E. and Piperno, G. (1988). Posttranslational modifications of alpha tubulin: detyrosination and acetylation differentiate populations of interphase microtubules in cultured cells. *J. Cell Biol.* **106**, 12113-12120.

Calaghan, S. C., Le Guennec, J. Y. and White, E. (2001). Modulation of Ca2+ signaling by microtubule disruption in rat ventricular myocytes and its dependence on the ruptured patch-clamp configuration. *Circ. Res.* **88**, E32-E37.

Centner, T., Yano, J., Kimura, E., McElhinny, A. S., Pelin, K., Witt, C. C., Bang, M. L., Trombitas, K., Granzier, H., Gregorio, C. C. et al. (2001). Identification of muscle specific ring finger proteins as potential regulators of the titin kinase domain. *J. Mol. Biol.* **306**, 717-726.

Chang, W., Webster, D. R., Salam, A. A., Gruber, D., Prasad, A., Eiserich, J. P. and Bulinski, J. C. (2002). Alteration of the C-terminal amino acid of tubulin specifically inhibits myogenic differentiation. *J. Biol. Chem.* **277**, 30690-30698.

Clark, K. A., McElhinny, A. S., Beckerle, M. C. and Gregorio, C. C. (2002). Striated muscle cytoarchitecture: an intricate web of form and function. *Annu. Rev. Cell Dev. Biol.* **18**, 637-706.

Dai, K. S. and Liew, C. C. (2001). A novel human striated muscle RING zinc finger protein, SMRZ, interacts with SMT3b via its RING domain. *J. Biol. Chem.* **276**, 23992-23999.

Gomez, A. M., Kerfant, B. G. and Vassort, G. (2000). Microtubule disruption modulates Ca(2+) signaling in rat cardiac myocytes. *Circ. Res.* **86**, 30-36.

Gotthardt, M., Hammer, R. E., Hubner, N., Monti, J., Witt, C. C., McNabb, M., Richardson, J. A., Granzier, H., Labeit, S. and Herz, J. (2003). Conditional expression of mutant M-line titins results in cardiomyopathy with altered sarcomere structure. *J. Biol. Chem.* **278**, 6059-6065.

Granger, B. L. and Lazarides, E. (1979). Desmin and vimentin coexist at the periphery of the myofibril Z disc. *Cell* **18**, 1053-1063.

Granzier, H. and Labeit, S. (2002). Cardiac titin: an adjustable multi-functional spring. *J. Physiol.* **541**, 335-342.

Gregorio, C. C. and Antin, P. B. (2000). To the heart of myofibril assembly. *Trends Cell Biol.* **10**, 355-362.

Gregorio, C. C. and Fowler, V. M. (1995). Mechanisms of thin filament assembly in embryonic chick cardiac myocytes: tropomodulin requires tropomyosin for assembly. *J. Cell Biol.* **129**, 683-695.

Gregorio, C. C., Trombitas, K., Centner, T., Komerer, B., Stier, G., Kunke, K., Suzuki, K., Obermayr, F., Hermann, B., Granzier, H. et al. (1998). The NH2 terminus of titin spans the Z-disc: its interaction with a novel 19-kDa ligand (T-cap) is required for sarcomeric integrity. *J. Cell Biol.* **143**, 1013-1027.

Grove, B. K., Kurer, V., Lehner, C., Doetschman, T. C., Perriard, J.-C. and Eppenberger, H. M. (1984). A new 185,000-dalton skeletal muscle protein detected by monoclonal antibodies. *J. Cell Biol.* **98**, 518-524.

Gundersen, G. G., Khawaja, S. and Bulinski, J. C. (1989). Generation of a stable, posttranslationally modified microtubule array is an early event in myogenic differentiation. *J. Cell Biol.* **109**, 2275-2288.

Gurland, G. and Gundersen, G. G. (1995). Stable, detyrosinated microtubules function to localize vimentin intermediate filaments in fibroblasts. *J. Cell Biol.* **131**, 1275-1290.

Gustafson, T. A., Bahl, J. J., Markham, B. E., Roeske, W. R. and Morkin, E. (1987). Hormonal regulation of myosin heavy chain and alpha-actin gene expression in cultured fetal rat heart myocytes. *J. Biol. Chem.* **262**, 13316-13322.

Gyoeva, F. K. and Gelfand, V. I. (1991). Coalignment of vimentin intermediate filaments with microtubules depends on kinesin. *Nature* **353**, 445-448.

Holtzer, H., Forry-Schaudies, S., Dlugosz, A., Antin, P. and Dubyak, G. (1985). Interactions between IFs, microtubules, and myofibrils in fibrogenic and myogenic cells. *Ann. New York Acad. Sci.* **455**, 106-125.

Infante, A. S., Stein, M. S., Zhai, Y., Borisy, G. G. and Gundersen, G. G. (2000). Detyrosinated (Glu) microtubules are stabilized by an ATP-sensitive plus-end cap. *J. Cell Sci.* **113**, 3907-3919.

Kano, Y., Fujimaki, N. and Ishikawa, H. (1991). The distribution and arrangement of microtubules in mammalian skeletal muscle fibers. *Cell Struct. Funct.* **16**, 251-261.

Kerfant, B. G., Vassort, G. and Gomez, A. M. (2001). Microtubule disruption by colchicine reversibly enhances calcium signaling in intact rat cardiac myocytes. *Circ. Res.* **88**, E59-E65.

Khawaja, S., Gundersen, G. G. and Bulinski, J. C. (1988). Enhanced stability of microtubules enriched in detyrosinated tubulin is not a direct function of detyrosination level. *J. Cell Biol.* **106**, 141-149.

Klein, I. (1983). Colchicine stimulates the rate of contraction of heart cells in culture. *Cardiovasc. Res.* **17**, 459-465.

Kreitzer, G., Liao, G. and Gundersen, G. G. (1999). Detyrosination of tubulin regulates the interaction of intermediate filaments with microtubules in vivo via a kinesin-dependent mechanism. *Mol. Biol. Cell* **10**, 1105-1118.

Labeit, S. and Kolmerer, B. (1995). Titins: giant proteins in charge of muscle ultrastructure and elasticity. *Science* **270**, 294-296.

Li, Z., Mericskay, M., Agbulut, O., Butler-Browne, G., Carlsson, L., Thornell, L. E., Babinet, C. and Paulin, D. (1997). Desmin is essential for the tensile strength and integrity of myofibrils but not for myogenic commitment, differentiation, and fusion of skeletal muscle. *J. Cell Biol.* **139**, 129-144.

Liao, G. and Gundersen, G. G. (1998). Kinesin is a candidate for cross-bridging microtubules and intermediate filaments. Selective binding of kinesin to detyrosinated tubulin and vimentin. *J. Biol. Chem.* **273**, 9797-9803.

Linke, W. A. and Granzier, H. (1998). A spring tale: new facts on titin elasticity. *Biophys. J.* **75**, 2613-2614.

Mangan, M. E. and Olmsted, J. B. (1996). A muscle-specific variant of microtubule-associated protein 4 (MAP4) is required in myogenesis. *Development* **122**, 771-781.

McElhinny, A. S., Kakinuma, K., Sorimachi, H., Labeit, S. and Gregorio, C. C. (2002). Muscle-specific RING finger-1 interacts with titin to regulate sarcomeric M-line and thick filament structure and may have nuclear functions via its interaction with glucocorticoid modulatory element binding protein-1. *J. Cell Biol.* **157**, 125-136.

Miller, M. K., Bang, M. L., Witt, C. C., Labeit, D., Trombitas, C., Watanabe, K., Granzier, H., McElhinny, A. S., Gregorio, C. C. and Labeit, S. (2003). The muscle ankyrin repeat proteins: CARP, ankrd2/Arpp and DARP as a family of titin filament-based stress response molecules. *J. Mol. Biol.* **333**, 951-964.

Milner, D. J., Weitzer, G., Tran, D., Bradley, A. and Capetanaki, Y. (1996). Disruption of muscle architecture and myocardial degeneration in mice lacking desmin. *J. Cell Biol.* **134**, 1255-1270.

Milner, D. J., Taffet, G. E., Wang, X., Pham, T., Tamura, T., Hartley, C., Gerdes, A. M. and Capetanaki, Y. (1999). The absence of desmin leads to cardiomyocyte hypertrophy and cardiac dilation with compromised systolic function. *J. Mol. Cell. Cardiol.* **31**, 2063-2076.

Milner, D. J., Mavroidis, M., Weisleder, N. and Capetanaki, Y. (2000). Desmin cytoskeleton linked to muscle mitochondrial distribution and respiratory function. *J. Cell Biol.* **150**, 1283-1298.

Mues, A., van der Fen, P. F., Young, P., Furst, D. O. and Gautel, M. (1998). Two Ig-like domains of the Z-disc portion of titin interact in a conformation-dependent way with telethonin. *FEBS Lett.* **428**, 111-114.

Nag, A. C., Krehel, W. and Cheng, M. (1986). Distributions of vimentin and desmin filaments in embryonic cardiac muscle cells in culture. *Cytobios* **45**, 195-209.

Nag, A. C. and Huffaker, S. K. (1998). Distribution and organization of desmin in cultured adult cardiac muscle cells: reflection on function. *J. Muscle Res. Cell Motil.* **19**, 887-895.

Obermann, W. M., Gautel, M., Steiner, F., van der Ven, P. F., Weber, K. and Furst, D. O. (1996). The structure of the sarcomeric M band: localization of defined domains of myomesin, M-protein, and the 250-kD carboxy-terminal region of titin by immunelectron microscopy. *J. Cell Biol.* **134**, 1441-1453.

Ojima, K., Lin, Z. X., Zhang, Z. Q., Hijikata, T., Holtzer, S., Labeit, S., Sweeney, H. L. and Holtzer, H. (1999). Initiation and maturation of I-Z-I bodies in the growth tips of transfected myotubes. *J. Cell Sci.* **112**, 4101-4112.

O'Neill, A., Williams, M. W., Resneck, W. G., Milner, D. J., Capetanaki, Y. and Bloch, R. J. (2002). Sarcomlemmal organization in skeletal muscle lacking desmin: evidence for cytokeratins associated with the membrane skeleton at costameres. *Mol. Biol. Cell* **13**, 2347-2359.

Perhonen, M., Sharp, W. W. and Russell, B. (1998). Microtubules are needed for dispersal of alpha-myosin heavy chain mRNA in rat neonatal cardiac myocytes. *J. Mol. Cell. Cardiol.* **30**, 1713-1722.

Pizon, V., Iakovenko, A., van Der Ven, P. F., Kelly, R., Fatu, C., Furst, D. O., Karsenti, E. and Gautel, M. (2002). Transient association of titin and myosin with microtubules in nascent myofibrils directed by the MURF2 RING-finger protein. *J. Cell Sci.* **115**, 4469-4482.

Rothen-Rutishauser, B. M., Ehler, E., Perriard, E., Messerli, J. M. and Perriard, J. C. (1998). Different behaviour of the non-sarcomeric cyoskeleton in neonatal and adult rat cardiomyocytes. *J. Mol. Cell. Cardiol.* **30**, 19-31.

Saitoh, O., Arai, T. and Obinata, T. (1988). Distribution of microtubules and other cytoskeletal filaments during myotube elongation as revealed by fluorescence microscopy. *Cell Tissue Res.* **252**, 263-273.

Sato, H., Nagai, T., Kuppuswamy, D., Narishige, T., Koide, M., Menick, D. R. and Cooper, G. T. (1997). Microtubule stabilization in pressure overload cardiac hypertrophy. *J. Cell Biol.* **139**, 963-973.

Schulze, E., Asai, D. J., Bulinski, J. C. and Kirschner, M. (1987). Posttranslational modification and microtubule stability. *J. Cell Biol.* **105**, 2167-2177.

Sorimachi, H., Kinbara, K., Kimura, S., Takahashi, M., Ishiura, S., Sasagawa, N., Sorimachi, N., Shimada, H., Tagawa, K., Maruyama, K. et al. (1995). Muscle-specific calpain, p94, responsible for limb girdle muscular dystrophy type 2A, associates with connectin through IS2, a p94-specific sequence. *J. Biol. Chem.* **270**, 31158-31162.

Spencer, J. A., Eliazer, S., Ilaria, R. L. Jr, Richardson, J. A. and Olson, E. N. (2000). Regulation of microtubule dynamics and myogenic differentiation by MURF, a striated muscle RING-finger protein. *J. Cell Biol.* **150**, 771-784.

Takahashi, M., Tsutsui, H., Tagawa, H., Igarashi-Saito, K., Imanaka-Yoshida, K. and Takeshita, A. (1998). Microtubules are involved in early hypertrophic responses of myocardium during pressure overload. *Am. J. Physiol.* **275**, H341-H348.

Takahaski, M., Shiraishi, H., Lshibashi, Y., Blade, K. L., McDermott, P. J., Menick, D. R., Kuppuswamy, D. and Cooper, G. (2003). Phenotypic consequences of beta-1 tubulin expression and MAP4 decoration of microtubules in adult cardiomyocytes. *Am. J. Physiol. Heart Circ. Physiol.* **285**, H2070-H2083.

Toyama, Y., Forry-Schaudies, S., Hoffman, B. and Holtzer, H. (1982). Effects of taxol and Colcemid on myofibrillogenesis. *Proc. Natl. Acad. Sci. USA* **79**, 6556-6560.

Tsutsui, H., Ishihara, K. and Cooper, G. T. (1993). Cytoskeletal role in the contractile dysfunction of hypertrophied myocardium. *Science* **260**, 682-687.

Webster, D. R., Wehland, J., Weber, K. and Borisy, G. G. (1990). Detyrosination of alpha tubulin does not stabilize microtubules in vivo. *J. Cell Biol.* **111**, 113-122.

Webster, D. R. (1997). Regulation of post-translationally modified microtubule populations during neonatal cardiac development. *J. Mol. Cell. Cardiol.* **29**, 1747-1761.

Webster, D. R. and Patrick, D. L. (2000). Beating rate of isolated neonatal cardiomyocytes is regulated by the stable microtubule subset. *Am. J. Physiol. Heart Circ. Physiol.* **278**, H1653-H1661.

Young, P., Ehler, E. and Gautel, M. (2001). Obscurin, a giant sarcomeric Rho guanine nucleotide exchange factor protein involved in sarcomere assembly. *J. Cell Biol.* **154**, 123-136.